

Dynamically Running Quadrupeds Self-Stable Region Expansion by Mechanical Design

Panagiotis Chatzakos and Evangelos Papadopoulos, *Senior Member, IEEE*

Abstract— Dynamic stability allows running animals to maintain preferred speed during locomotion over rough terrain. It appears that rapid disturbance rejection is an emergent property of the mechanical system. In running robots, simple motor control seems to be effective in the negotiation of rough terrain when used in concert with a mechanical system that stabilizes passively. In this paper, we show that a quadruped robot could be able to perform self-stable running behavior in significantly broader ranges of forward speed and pitch rate with suitable mechanical design. The results presented here are derived by studying the stability of passive dynamics of a quadruped robot running in the sagittal plane in a dimensionless context and can be summarized as: (a) the self-stabilized behavior of a quadruped robot for a particular gait is related to the magnitude of its dimensionless inertia, (b) the values of hip separation, normalized to rest leg length, and the leg relative stiffness of a quadruped robot affect the stability and should be in inverse proportion to its dimensionless inertia, and (c) the self-stable regime of quadruped running robots is enlarged at relatively high forward speeds.

I. INTRODUCTION

Negotiation of rough terrain is the most important reason for building legged robots, as opposed to wheeled and tracked ones. Animals exhibit impressive performance in handling rough terrain and hence they can reach a much larger fraction of the earth landmass on foot than wheeled vehicles. Their robotic counterparts have not yet been benefited from the improved mobility and versatility that legs offer. Early attempts to design legged platforms resulted in slow, statically stable robots, which are still the most prevalent today; see [1] for a survey.

In this paper, however, we focus on dynamically stable legged robots. Two decades ago, Raibert set the stage with his groundbreaking work on dynamic legged locomotion by introducing very simple controllers for stabilizing running on one-, two- and four-legged robots, [2]. Later on, Buehler designed and built power autonomous legged robots with one, four and six legs, which demonstrate running in a dynamic fashion, [3]. Tekken robotic quadruped by Kimura

and co-workers is an example of another design and control approach for dynamically stable running based on neurobiological principles, [4].

Despite their morphological and design differences, all these robots are propelled forward using control laws without intense feedback. For instance, Poulakakis et al. on quadrupedal robot Scout II demonstrated recently that simple controllers, requiring only touchdown detection and local feedback from motor encoders, can be used to stabilize running, [5]. These controllers simply position the legs at a fixed touchdown angle during the flight phase and result in stable bounding.

In a loose sense, these experimental findings in robotics are in qualitative agreement with developments in biology. As experimental evidence suggests, high level nervous system is not required for steady state level running, and mechanisms entirely located within the spinal cord are responsible for generating the rhythmic motions of legs during locomotion; see [6] and [7]. Further, control during rapid locomotion is dominated by the mechanical system as recent research in physiology indicates; see [8] and [9].

In this paper, motivated by the experimental findings in existing robots, we investigate whether the self-stable regions of complex running tasks, such as bounding, can be enlarged. Our analysis departs from the recent developments regarding the self-stabilization property of quadruped robots, such as SCOUT II by Poulakakis et al., where it is shown that the dynamics of the open loop passive system alone can confer stability of the motion, [10]. It was found that bounding gaits can be passively generated as a response of the system to an appropriate set of initial conditions and a regime where the system is self-stabilized against small perturbations from the nominal conditions was identified. However, this regime involved running with forward speeds of 3-4 m.s⁻¹ and bounding with 100-200 deg.s⁻¹ (pitch rate), which is not practically achievable with existing quadruped robots.

In our work, however, stability analysis of the passive dynamics of quadruped robots is studied in a dimensionless context, inspired by the approach followed in [11], revealing further intrinsic properties and unveiling aspects of quadrupedal running. It is shown that proper selection of robot physical parameters can provide self-stable running behavior in significantly broader ranges of forward speed and pitch rate, which are, most importantly, physically realistic. We anticipate the proposed guidelines to assist in

This work is co-funded by public (European Social Fund 80% and General Secretariat for Research and Technology 20%) and private funds (Zenon SA), within measure 8.3 of Op. Pr. Comp., 3rd CSP-PENED'03.

Panagiotis Chatzakos is with the Department of Mechanical Engineering, National Technical University of Athens, Greece (phone: +30-697-746-7158; e-mail: pchatzak@mail.ntua.gr).

Evangelos Papadopoulos is with the Department of Mechanical Engineering, National Technical University of Athens, Greece (phone: +30-210-772-1440; fax: +30-210-772-1450; e-mail: egpapado@central.ntua.gr).

the design of new, and the modification of existing robotic quadrupeds.

II. SYSTEM MODELING

In this section we introduce a simple model for studying and analyzing gaits where pitching motion is a significant mode in the system's motion, e.g. bounding. Inspired by the Spring Loaded Inverted Pendulum (SLIP) model, which exhibits natural stability, we aim at identifying a template for studying the dynamics of gaits with body pitching. Note that the bound cannot be studied using the SLIP since it does not capture body's oscillatory motion.

The fact that bounding is essentially a natural mode of the system, and that only minor control and energy effort are required to maintain running, practically motivated us to study the passive dynamics of the system, which is the unforced response of the system under a set of initial conditions. This unactuated and conservative model is shown in Fig. 1, while its parameters are given in Table 1.

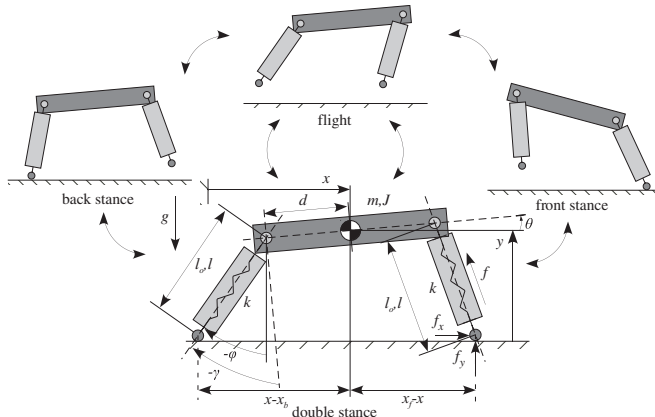


Figure 1. The template for quadrupedal running in plane and gait phases.

TABLE 1.
VARIABLES AND INDICES USED.

Symbol	Variable	Symbol	Variable
x	COM horizontal pos.	g	acceleration of gravity
y	COM vertical pos.	m	body mass
θ	body pitch angle	J	body inertia
γ	leg absolute angle	d	hip to COM distance
φ	leg relative angle	f	as an index: front leg
x_{bt}	back toe horizontal pos.	b	as an index: back leg
x_{ft}	front toe horizontal pos.	j	dimensionless inertia
l	leg length	r	relative leg stiffness
l_0	leg rest length	p	half hip separation
k	leg spring stiffness	Fr	Froude number
f	axial force at leg	s	time scale
h_{apex}	flight apex position	*	dimensionless

As shown in Fig. 1, the planar model represents the lateral half of a quadruped, and consists of a rigid body and two springy massless legs, attached to either side of the body. Actuators control the angle of each leg with respect to the body. Each modeled leg represents the back or the front leg pair, in which the two back or front legs are always in phase and is called the virtual leg, [2]. Each virtual leg has

twice the stiffness of the robot leg.

System dynamics are derived using a Lagrangian formulation, with generalized coordinates to be the Cartesian variables describing the center of mass (COM) position and main body attitude. During flight, the robot is under the influence of gravity only. Throughout stance phase, robot's toes are fixed on the ground, and act as lossless pivot joints.

The resulting set of equations is manipulated next to be independent of the choice of units, i.e. dimensionless. The non-dimensional variables are formed in ways that define the morphology of the quadruped robot or that correspond to ratios of robot physical parameters in the model equations. To achieve that, the following dimensionless variables are introduced,

$$t^* = t/s \quad (1)$$

$$x^* = x/l_o, \dot{x}^* = s \dot{x}/l_o, \ddot{x}^* = s^2 \ddot{x}/l_o \quad (2)$$

$$y^* = y/l_o, \dot{y}^* = s \dot{y}/l_o, \ddot{y}^* = s^2 \ddot{y}/l_o \quad (3)$$

$$\theta^* = \theta, \dot{\theta}^* = s \dot{\theta}, \ddot{\theta}^* = s^2 \ddot{\theta} \quad (4)$$

where s is the time scale of the system, while the rest of the variables are defined in Table 1.

By substituting (1)-(4) into the equations of motion one gets a dimensionless description of the system. The resulting motion of the COM is then characterized by a time scale, which is associated to the inverse of the natural frequency of the horizontal motion,

$$s^2 g/l_o = 1 \Rightarrow s = \sqrt{l_o/g} \quad (5)$$

While the individual dimensionless equations would be different if one uses another time scale, the relationships between them would be invariant.

Selection of the time scale as in (5), results to a number of dimensionless parameter groups, which are widely used by experimental biologists. These include: (a) Froude number Fr ([5]), defined as

$$Fr = v/\sqrt{g l_o} \quad (6)$$

where v is the robot forward speed, (b) dimensionless inertia j ([12]), i.e. robot body inertia normalized to md^2 ,

$$j = J/md^2 \quad (7)$$

and (c) leg relative stiffness r ([13]), which is given as

$$r = k l_o/mg. \quad (8)$$

Also, the normalized half hip separation p is introduced,

$$p = d/l_o, \quad (9)$$

while force variables are normalized as

$$f_i^* = f_i/mg, i = b, f. \quad (10)$$

The sought-after dimensionless description of the system is given by (11)-(15) for the double stance, in the form of a set of differential and algebraic equations,

$$\dot{x}^* = -r(1-l_b^*)\sin\gamma_b^* - r(1-l_f^*)\sin\gamma_f^* \quad (11)$$

$$\ddot{y}^* = r(1-l_b^*)\cos\gamma_b^* + r(1-l_f^*)\cos\gamma_f^* - 1 \quad (12)$$

$$\ddot{\theta} = r \left((1-l_f^*) \cos \phi_f^* - (1-l_b^*) \cos \phi_b^* \right) / p j \quad (13)$$

where

$$\gamma_b^* = \text{Atan2}(y^* - p \sin \theta^*, x_{bt}^* + p \cos \theta^* - x^*) \quad (14)$$

$$\gamma_f^* = \text{Atan2}(y^* + p \sin \theta^*, x_{ft}^* - p \cos \theta^* - x^*)$$

$$l_b^* = \sqrt{(x_{bt}^* - x^* + p \cos \theta^*)^2 + (p \sin \theta^* - y^*)^2} \quad (15)$$

$$l_f^* = \sqrt{(x_{ft}^* - x^* - p \cos \theta^*)^2 + (p \sin \theta^* + y^*)^2}$$

The dynamics for any other phase may be derived from that of the double stance, by removing appropriate terms.

III. STABILITY ANALYSIS

The goals of analysis are to determine the conditions required to permit steady state cyclic motion and find ways to apply these results to facilitate improved quadruped robots design. System periodic steady state trajectories are identical trajectories that repeat themselves during one cycle of locomotion. To formulate these trajectories, we employ a Poincaré Map technique, which connects system state at a well-defined locomotion event to state of the same event at the next cycle.

This event is chosen here to be apex height, because the vertical velocity at apex height is always zero, which reduces the dimensions of the state vector. A second dimensional reduction to the state vector can be obtained by projecting out the horizontal component x of the state vector, since it is not relevant to describing the running gait. Thus, the state vector \mathbf{x}^* at apex height is given as,

$$\mathbf{x}^* = [y^* \quad \theta^* \quad \dot{x}^* \quad \dot{\theta}^*]. \quad (16)$$

The state vector at apex height for some cycle n , \mathbf{x}_n^* , constitutes the initial conditions. Based on these, the flight equations are integrated until one of the touchdown events occurs, e.g., front or back leg stance. The touchdown event triggers the next phase, whose dynamics are integrated using as initial conditions the final conditions of the previous state. Successive forward integration of the dynamic equations of all the phases yields the state vector at apex height of the next stride, which is the value of the Poincaré return map \mathbf{F} . If the state vector at the new apex height is identical to the initial one, the cycle is repetitive and yields a fixed point. Mathematically, this is given as

$$\mathbf{x}_{n+1}^* = \mathbf{F}(\mathbf{x}_n^*, \mathbf{u}_n^*) \quad (17)$$

where \mathbf{u}^* includes the inputs, which is the vector of touchdown angles, back and front leg,

$$\mathbf{u}^* = [\gamma_{b,td}^* \quad \gamma_{f,td}^*] \quad (18)$$

Despite the fact that touchdown angles are not part of the state vector and they do not participate in the dynamics, they directly affect the value of return map as they determine touchdown and liftoff events and impose constraints on the motion of robot during stance phases.

In order to determine the conditions required to result in steady state cyclic motions, we resort to a numerical evaluation of the return map using a Newton-Raphson method. By employing this method, a large number of fixed points can be found for different initial conditions and inputs. Variant dimensionless combinations of robot's physical parameters, as defined in (7)-(9), also result to different fixed points. These design parameters vary between their extreme values found in experimental biology references, [14], as follows,

$$j = 0.70 - 1.45, \quad r = 10 - 30, \quad p = 0.25 - 1.00 \quad (19)$$

The existence of passively generated running cycles is by itself a very important result since it shows that such a complex activity can be simply a natural motion of the system. However, in real situations the robot is continuously perturbed, therefore, if the fixed point were unstable, then the periodic motion would not be sustainable. Hence, it is important to study the stability properties of fixed points found above and to identify robot physical parameters that improve robustness of system against perturbations. We characterize the stability of fixed points using the eigenvalues of the linearized return map. For that, we assume that the apex height states are perturbed from their steady-cycle values $\bar{\mathbf{x}}$, by some small amount $\Delta \mathbf{x}$. The model that relates the deviations from steady state, i.e. the incremental or small-signal model, is

$$\Delta \mathbf{x}_{n+1}^* = \partial \mathbf{F}(\mathbf{x}^*, \mathbf{u}^*) / \partial \mathbf{x} \Big|_{\bar{\mathbf{x}}} \Delta \mathbf{x}_n^* + \partial \mathbf{F}(\mathbf{x}^*, \mathbf{u}^*) / \partial \mathbf{u} \Big|_{\bar{\mathbf{u}}} \Delta \mathbf{u}_n^* \quad (20)$$

with $\Delta \mathbf{x} = \mathbf{x}^* - \bar{\mathbf{x}}$ and $\Delta \mathbf{u} = \mathbf{u}^* - \bar{\mathbf{u}}$. For small perturbations, the apex height states at the next stride can be calculated by (20), which is a linear difference equation. If all the eigenvalues of the system matrix \mathbf{A} ,

$$\mathbf{A} = \partial \mathbf{F}(\mathbf{x}^*, \mathbf{u}^*) / \partial \mathbf{x} \Big|_{\bar{\mathbf{x}}} \quad (21)$$

have magnitude less than one, then the periodic solution is stable and disturbances decay in subsequent steps. If not, then they grow and eventually repetitive motion is lost.

IV. RESULTS & GUIDELINES

Using this systematic procedure for finding stable fixed points described previously, conclusions on how the system responds under a set of initial conditions and design parameters can be drawn. Surprisingly, there are parametric regions where the system is stable and can passively tolerate departures from the fixed points. The purpose of this section is to quantify the properties of passively generated periodic motion for quadruped robots.

To demonstrate how motion characteristics and design parameters affect the stability of the motion, we present figures that display isolines of the magnitude of the larger eigenvalue of system matrix \mathbf{A} , as defined in (21). The largest eigenvalue norm is interpreted as heights with respect to the x-y plane, where x-y variables are either motion characteristics, such as forward speed and pitch rate,

or the dimensionless combinations of robot physical parameters defined in (7)-(9), e.g. dimensionless inertia, leg relative stiffness and normalized half hip separation. For certain values of these variables the larger eigenvalue enters the unit circle, while the other eigenvalues remain well behaved. This fact shows that, for these parameter values, the system is self-stabilized. In all figures, the grey hatched area corresponds to unstable regions, i.e., regions where at least one eigenvalue is located outside of the unit circle and the system is not passively stable. The magnitude of the “non-participating” variables is shown in the title of each subplot in every figure.

To this end, isolines of the largest eigenvalue norm at various pitch rates and values of dimensionless inertia are displayed in Fig. 2. The contour plots are drawn for dimensionless apex height 1.1, leg relative stiffness 12, and normalized half hip separation 0.85. The magnitude of these variables has been chosen such as to correspond to the physical parameters of Scout II, [10]. The reason for this choice is to demonstrate how an existing robot can be mechanically modified in order to expand the domain of attraction of its self-stabilized behavior.

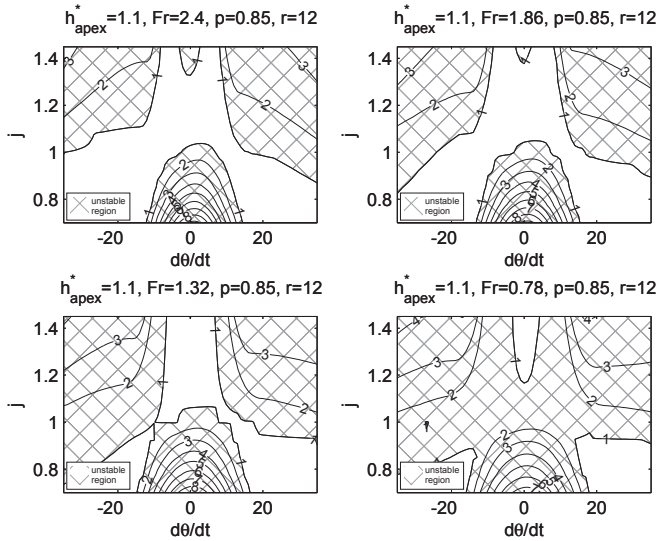


Figure 2. Largest eigenvalue norm at various pitch rates and dimensionless inertias and forward speeds.

The main conclusion from the analysis performed by Poulakakis et al. is that there exists a regime where the Scout II robot can be passively stable, [10]. Similar findings are evident in Fig. 2, where the four subplots have been plotted for dimensionless forward speeds (Froude number) from 2.40 to 0.78. For the particular mechanical design adopted for the Scout II robot, the self-stable regime, where all the eigenvalues lie inside the unit circle, is achieved for bounding at sufficiently high forward speeds. This was also reported in [10].

However, as it can be deduced by Fig. 2, by changing the value of dimensionless inertia, the Scout II robot can expand its self-stable regime and passively bound at

surprisingly lower forward speeds. It is simple for a robot to attain a specific value of dimensionless inertia by proper hip placement or redistributing body mass.

Finding 1. Large forward speed favors the self-stabilized behavior of quadruped robots, as it enlarges the regime where the mechanical system can reject rapid perturbations. When the quadruped robot is moving more slowly, the magnitude of dimensionless inertia must take extreme values in order to sustain the self-stabilizing characteristics; greater than one for low pitch rates and less than one for high pitch rates.

According to Poulakakis et al. ([10]) the largest eigenvalue obtained its maximum value when the pitch rate was small. Recall that the region where pitch rate takes small values corresponds to a pronking-like motion, where both the front and back legs hit and leave the ground in unison and pitch rate is minimized. Thus, they had concluded that pronking-like motions (low pitch rates) are “more unstable” than bounding (high pitch rates). This fact was also observed in experiments with the Scout II. As seen in Fig. 2, this is true when the dimensionless inertia is less than one. However, attaining a value of dimensionless inertia that is greater than one could provide to Scout II robot self-stabilizing characteristics for pronking motions, as well. Note that the lower the forward speed, the greater the value of dimensionless inertia must be.

The dimensionless moment of inertia, see [12] for definition, describes the “resistance” to rotational versus the “resistance” to translational motion, due to the mass distribution. In a diagrammatic manner, dimensionless inertia can be thought of as two equal point masses that represent the total mass of the system concentrated at the hips of the torso for the case of unit dimensionless inertia ($J=md^2$), located between the hips for the case dimensionless inertia greater than one ($J>md^2$) and located outside the hips for the case dimensionless inertia less than one ($J<md^2$). Note that the distance from the COM at which the point masses are located is the radius of gyration. Therefore, depending on the location of the equivalent point masses, i.e. the magnitude of dimensionless moment of inertia, pronking-like motion, where pitch motion is negligible, or bounding, where the pitch motion is dominant, is favored.

Finding 2. The self-stabilized behavior of a quadruped robot for a particular gait is related to the magnitude of its dimensionless inertia. Dimensionless inertia less than one provides self-stabilizing characteristics for bounding motions (high pitch rates), while pronking-like motions (low pitch rates) are self-stable for quadruped robots with dimensionless inertia greater than one.

The effect of normalized half hip separation is depicted in Fig. 3, as four subplots have been plot for normalized half hip separation from 0.325 to 1.000. As in Fig. 2,

isolines of the largest eigenvalue norm at various pitch rates and dimensionless inertias are displayed in Fig. 3. The contour plots are drawn for dimensionless apex height 1.1, dimensionless forward speed (Froude number) 2.04 and leg relative stiffness 12, which are again adopted from the Scout II robot.

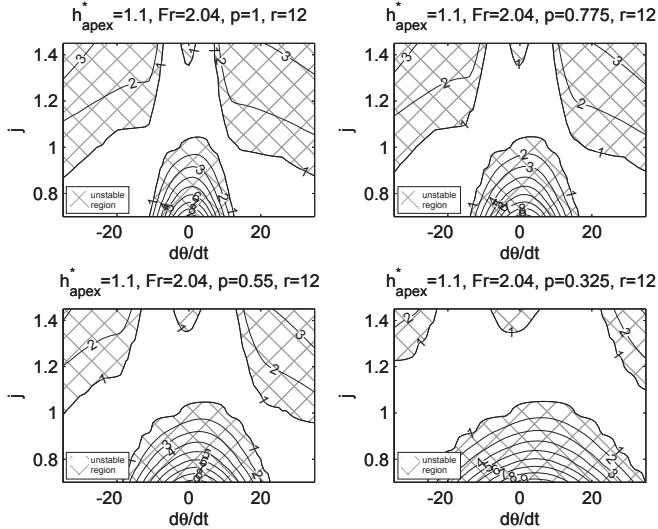


Figure 3. Largest eigenvalue norm at various pitch rates and dimensionless inertias and half hip separations.

The main conclusion drawn by analyzing Fig. 3 is that the self-stabilized regime of the quadruped robot is enlarging when the normalized half hip separation is decreasing. Decreased normalized half hip separation simply means that body length is smaller for the same leg length. Small body length results to increased “resistance” to rotational motion compared to translational motion, i.e. the hip will move upwards due to linear acceleration instead of moving downwards due to rotational acceleration. In this case, pitch motion is not favoured and pronking-like motions dominate. For the Scout II robot, for which the “resistance” against rotational motion is smaller than that against translational motion (dimensionless inertia less than one, i.e. $J < md^2$), dimensionless hip separation should be as large as possible to allow for self-stable bounding at lower (practically achievable) pitch rates, which is easy to achieve by proper hip placement.

One may reach the same conclusion by analyzing Fig. 4 and Fig. 5, where the contour plots of the largest eigenvalue norm at various pitch rates and values of leg relative stiffness are drawn. Once again, the magnitude of the variables has been chosen such as to correspond to the physical parameters of Scout II robot. Specifically, the dimensionless apex height is 1.1 and the dimensionless forward speed (Froude number) is 2.04. In Fig. 4, the dimensionless inertia is 0.850, as in Scout II, while in Fig. 5 the dimensionless inertia is chosen to be 1.225 to demonstrate the effect of relative leg stiffness on quadruped robots with dimensionless inertia greater than one. The

effect of normalized half hip separation is represented graphically by Fig. 4 and Fig. 5, as the four subplots in each figure have been plotted for normalized half hip separation from 0.325 to 1.000.

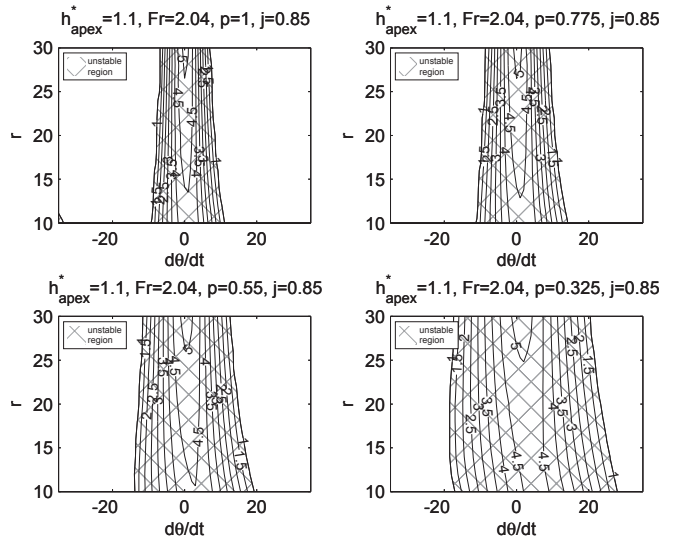


Figure 4. Largest eigenvalue norm at various pitch rates and leg relative stiffnesses and half hip separations.

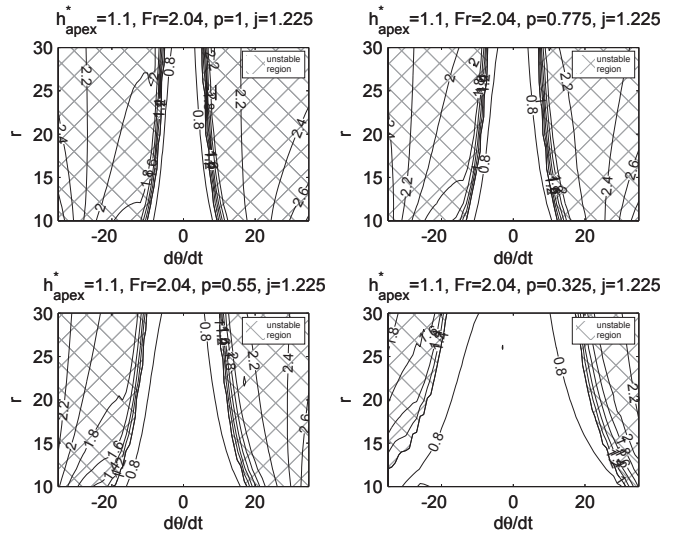


Figure 5. Largest eigenvalue norm at various pitch rates and leg relative stiffnesses and half hip separation.

In Fig. 4, it is evident that the self-stabilized regime of bounding quadruped robots with dimensionless inertia less than one is enlarging while the normalized half hip separation is increasing. Contrastingly, as Fig. 5 implies, normalized half hip separation should be decreased for quadruped robots with dimensionless inertia greater than one that pronk or bound at low pitch rates so as to enlarge their self-stabilized regime. A specific value of hip separation is easily attained by proper hip placement.

Finding 3. The self-stabilized regime of pronking-like motions (low pitch rates) for quadruped robots with dimensionless inertia greater than one is enlarging while

the normalized half hip separation is decreasing. Larger dimensionless hip separation allows for self-stable bounding at a wider range of pitch rates for quadruped robots with dimensionless inertia less than one.

With respect to the effect of leg relative stiffness on the stability of the motion and the self-stabilizing characteristics of the robot, two conclusions are drawn by analyzing Fig. 4 and Fig. 5. Based on Fig. 4, the self-stabilized regime of bounding quadruped robots with dimensionless inertia less than one is enlarging while the relative leg stiffness is increasing. Contrastingly, based on Fig. 5, relative leg stiffness should be decreased for quadruped robots with dimensionless inertia greater than one that pronk or bound at low pitch rates so as to enlarge their self-stabilized regime.

The former can be explained by the fact that harder springs at legs, a typical case where leg relative stiffness is increased, result to less compression along the leg during leg-ground interaction, which typically leads to less pitching. Since the “resistance” against rotational motion is smaller than the “resistance” against translational motion when $J < md^2$ (dimensionless inertia less than one), self-stable motions at lower pitch rate are possible; see Fig. 4 to graphically visualize this.

On the other hand, leg relative stiffness is increased when the mass of the system is decreased in a proportional manner; see (8) for definition. Smaller mass means that the “resistance” against translational motion is less or equivalently that the “resistance” against rotational motion is dominant. In that case, i.e. for quadruped robots with dimensionless inertia less than one ($J > md^2$), lower pitch rates are required to allow for self-stabilizing behavior; see Fig. 5 for depiction.

Finding 4. Leg relative stiffness for a quadruped robot should be chosen according to the magnitude of the dimensionless inertia. Dimensionless inertia less than one suggests that relative leg stiffness should be as large as possible to enlarge the self-stable regime of the system. Contrastingly, relative leg stiffness should be decreased for quadruped robots with dimensionless inertia greater than one that pronk (or bound at low pitch rates) so as to enlarge their self-stabilized regime.

Taking into account the above mentioned findings, the following design guidelines could be proposed for Scout II quadruped robot that might improve its performance:

(1) Scout II would passively bound at lower forward speeds by changing the value of its dimensionless inertia. By attaining a value of dimensionless inertia that is greater than one, it would obtain self-stabilizing characteristics even for pronking-like motions. This is easily attained by proper hip placement or body mass redistribution.

(2) Scout II would be able to perform self-stable bounding behavior at lower and practically achievable pitch rates,

even if its dimensionless inertia is kept less than one, by increasing its normalized hip separation. This could be easily achieved either by proper hip placement or by shortening its legs rest length.

(3) The self-stabilized regime of the existing Scout II bounding robot could be further enlarged if its legs relative stiffness is increased, which could be attained simply by increasing its legs spring stiffness or by shortening their rest length.

V. CONCLUSION

Stability analysis of passive dynamics of robotic quadrupeds was studied in a dimensionless context. It was shown that mechanical design can provide self-stabilizing characteristics to a quadruped robot against external perturbations and result to dynamically stable running with bounding and pronking-like gaits with physically realistic forward speeds and pitch rates. We anticipate that the proposed guidelines will assist in the design of new, and modification of existing quadruped robots. These can be summarized as: (a) greater forward speeds enlarge the self-stable regime of quadruped running robots, (b) the self-stabilized behavior of a quadruped robot for a particular gait is roughly related to the magnitude of its dimensionless inertia, and (c) the values of normalized hip separation and leg relative stiffness affect the stability of quadruped running robot and should be in inverse proportion to its dimensionless inertia.

REFERENCES

- [1] Berns K., Walking Machine Catalogue, www.walking-machines.org.
- [2] Raibert M. H., “Legged Robots that Balance”, MIT Press, Cambridge, MA, 1986.
- [3] Buehler M., “Dynamic Locomotion with One, Four and Six-Legged Robots”, Journal of the Robotics Society of Japan, 20(3): 15-20, 2002.
- [4] Kimura, Fukuoka H. Y. and Cohen A. H., “Adaptive Dynamic Walking of a Quadruped Robot on Natural Ground Based on Biological Concepts”, Int. Journal of Robotics Research, 26(5):475-490, 2007.
- [5] Alexander R. McN., “Terrestrial Locomotion”, Mechanics and Energetics of Animal Locomotion, Chapman and Hall, London, 1977.
- [6] McMahon T., “Muscles, Reflexes, and Locomotion”, Princeton University Press, 1985.
- [7] Pearson K., “Control of Walking”, Scientific American. 72:86, 1976.
- [8] Kubow T. and Full R., “The Role of the Mechanical System in Control: A Hypothesis of Self-stabilization in Hexapedal Runners”, Phil. Trans. of Royal Society of London, 354(1385):854-862, 1999.
- [9] Full R. J. and Koditschek D., “Templates and Anchors: Neuro-mechanical Hypotheses of Legged Locomotion on Land”, Journal of Experimental Biology, 202:3325-3332, 1999.
- [10] Poulakakis, I. Papadopoulos E. G. and Buehler M., “On the Stability of the Passive Dynamics of Quadrupedal Running with a Bounding Gait”, International Journal of Robotics Research, 25(7):669-687, 2006.
- [11] Chatzacos, P. and Papadopoulos, E., “Bio-Inspired Design of Electrically-Driven Bounding Quadrupeds via Parametric Analysis”, Mechanisms and Machine Theory, 44(3):559-579, 2009.
- [12] Murphy K. and Raibert M., “Trotting and Bounding in a Planar Two-legged Model”, 5th Symposium on Theory and Practice of Robots and Manipulators, MIT Press, Cambridge MA, pp: 411-420, 1984.
- [13] Blickhan R., “The spring-mass model for running and hopping”, Journal of Biomechanics, 22: 1217-1227, 1989.
- [14] Farley C.T., Glasheen J., and McMahon T.A., “Running springs: speed and animal size”, J. of Experimental Biology, 185(1):71-86, 1993.